Journal of Asian Earth Sciences 284 (2025) 106565

Contents lists available at ScienceDirect

Journal of Asian Earth Sciences

journal homepage: www.elsevier.com/locate/jseaes

Thermo-rheological structure of the lithosphere in Hainan Island, Southeast China and its geothermal significance

Kefu Li [a,b], Chuanqing Zhu [a,b,*], Mengfei Zhang [a,b], Shudi Xing [a,b], Yanyu Jia [a,b,c], Chenxing Li [a,b]

[a] State Key Laboratory of Petroleum Resources and Engineering, China University of Petroleum (Beijing), Beijing 102249, China
[b] College of Geoscience, China University of Petroleum (Beijing), Beijing 102249, China
[c] Sinopec Star Petroleum Co., Ltd., Beijing 100083, China

ARTICLE INFO

Keywords:
Thermal structure
Lithosphere
Rheological structure
Hainan Island

ABSTRACT

Based on heat flow, seismic wave velocity, and rheological parameter data, this study constructs a thermo-rheological model of the lithosphere beneath Hainan Island, China. Using this model, we have determined the thermal structure, thermal lithosphere thickness, and rheological structure of the lithosphere beneath Hainan Island. The results indicate a "cold crust, hot mantle" thermal structure, with mantle heat flow ranging from 49 to 58 mW/m^2, contributing over 65 % of the total heat flow. Hainan Island exhibits a relatively thin thermal lithosphere that gradually thickens from north to south, and characterized by a high surface heat flow with corresponding changing trends. The rheological structure of Hainan Island follows a "brittle-ductile–brittle-ductile" pattern, characteristic of a "strong crust and weak mantle" configuration. Our analysis suggests that the high thermal state/condition and unique thermo-rheological structure of Hainan Island are closely related to the geodynamic background of Pacific plate subduction and the upwelling of the Hainan mantle plume. This upwelling has led to the formation of a high-temperature anomaly zone in the upper mantle beneath the island. Additionally, the thermal structure of the lithosphere significantly controls its rheological strength, with terrestrial heat flow influencing the regional strength of the lithosphere.

1. Introduction

The thermal structure of the lithosphere reflects its evolutionary process and exerts a significant influence on the entire lithospheric evolution (He et al., 2001; Tang et al., 2018). Analysis of the lithospheric thermal structure primarily focuses on the "crust-mantle" heat flow ratio, temperature distribution with depth, and lithospheric thickness (Yang and Li, 2022; Zang et al., 2002; Liu et al., 2005; Huang et al., 2015). The thermo-rheological structure of the lithosphere can explain deformation behaviors within it and facilitates understanding of dynamic evolutionary processes in basins, continental margins, and orogenic belts. Furthermore, it plays a crucial role in studying deep continental thermal processes, hydrocarbon thermal maturity, and seismic source mechanisms (Qiu et al., 2017; Tesauro et al., 2009; Liu et al., 2003).

Hainan Island is situated at the intersection of the Pacific Plate, Philippine Sea Plate, and Indo-China Plate. Extensive magmatic activities across multiple phases have led to the widespread distribution of magmatic rocks on the island. Previous measurements of terrestrial heat flow in Hainan Island have shown that the average heat flow value exceeds that of the Chinese mainland by 62 mW/m^2 (Chen et al., 1991; Hu et al., 2001), indicating significant potential for geothermal resources. Currently, over 40 geothermal fields and hot springs have been identified on Hainan Island, primarily concentrated in the central and southern regions where heat flow values are even higher. Hydrothermal geothermal resources in these areas are currently the primary targets for exploitation and development, while hot dry rock geothermal resources also exhibit considerable potential (Chen, 2008; Gao et al., 2009; Zhao, 2016; Zhang et al., 2018, 2024; Zhang, 2020). Yun et al. (2023) suggest the potential existence of hot dry rock reservoirs in the Lingshui area of southern Hainan Island, with heat sources likely originating from radiogenic heating within granite and mantle heat flow. Shi (2015) proposed that deep-layer temperatures of geothermal fields in the Qiongbei Basin in northern Hainan Island may be dominated by mantle heat sources. Based on current research, Hainan Island is abundant in geothermal resources. However, the causes of its high heat flow and the

* Corresponding author at: State Key Laboratory of Petroleum Resources and Engineering, China University of Petroleum (Beijing), Beijing 102249, China.
E-mail addresses: likefu553@163.com (K. Li), zhucq@cup.edu.cn (C. Zhu).

https://doi.org/10.1016/j.jseaes.2025.106565
Received 13 November 2024; Received in revised form 27 January 2025; Accepted 12 March 2025
Available online 16 March 2025

genesis of these geothermal resources remain unclear. Therefore, this study focuses on Hainan Island as the study area, integrating regional geophysical data and employing inversion techniques to reveal the characteristics of the lithospheric thermal structure and thermo-rheological structure. This research provides insights into the theoretical development of geothermal resource formation and offers valuable references for geothermal resource exploration and development on Hainan Island.

2. Geological setting

Hainan Island, situated in the northwest of the South China Sea and separated from the Chinese mainland by the Qiongzhou Strait, occupies a unique tectonic position at the juncture of the Pacific Plate, the Philippine Sea Plate, and the South China and Indochina Plates. Consequently, it exhibits complex tectonic features and a prolonged geological evolution history (Fig. 1a). Regarding the tectonic unit division of Hainan Island, various viewpoints exist within the academic community (Xia et al., 1991; Metcalfe et al., 1996; Chao et al., 2016). This study adopts the scheme proposed by Lei et al. (2024), which divides the island into three second-order tectonic units from north to south: the Leiqiong Rift Depression, the Wuzhishan Fold Belt, and the Sanya Platform Margin Depression, delineated by the Wangwu-Wenjiao Fault Zone and the Jiusuo-Lingshui Fault Zone. Within the Wuzhishan Fold Belt, the NE-trending Ding'an-Ledong Fault Zone further subdivides it into two third-order tectonic units: the Baoban Uplift and the Wuzhishan Uplift (Fig. 1b).

Hainan Island has experienced multiple intense tectonic activities and significant magmatic activity, resulting in the formation of a vast quantity of magmatic rocks from different geological periods. Magmatic rocks are widely distributed on the island, with intrusive rocks covering approximately 51 % of its total area, primarily concentrated south of the Wangwu-Wenjiao Fault. The most prominent intrusive rocks are Hercynian-Indosinian (Permian to Triassic) granites, followed by Yanshanian granites. Volcanic rocks account for about 13 % of the island's area, mainly distributed north of the Wangwu-Wenjiao Fault, with Cenozoic basalt as the dominant type (Wang et al., 2019; Zhou et al., 2021; Shi et al., 2022; Qi et al., 2023). Additionally, terrestrial heat flow values on Hainan Island range from 60 to 92 mW/m2, averaging over 70 mW/m2, exhibiting moderate to high regional terrestrial heat flow characteristics compared to typical craton-type continental and oceanic regions globally (Chen et al., 1991; Hu et al., 2001; Lei et al., 2023; Gao et al., 2020).

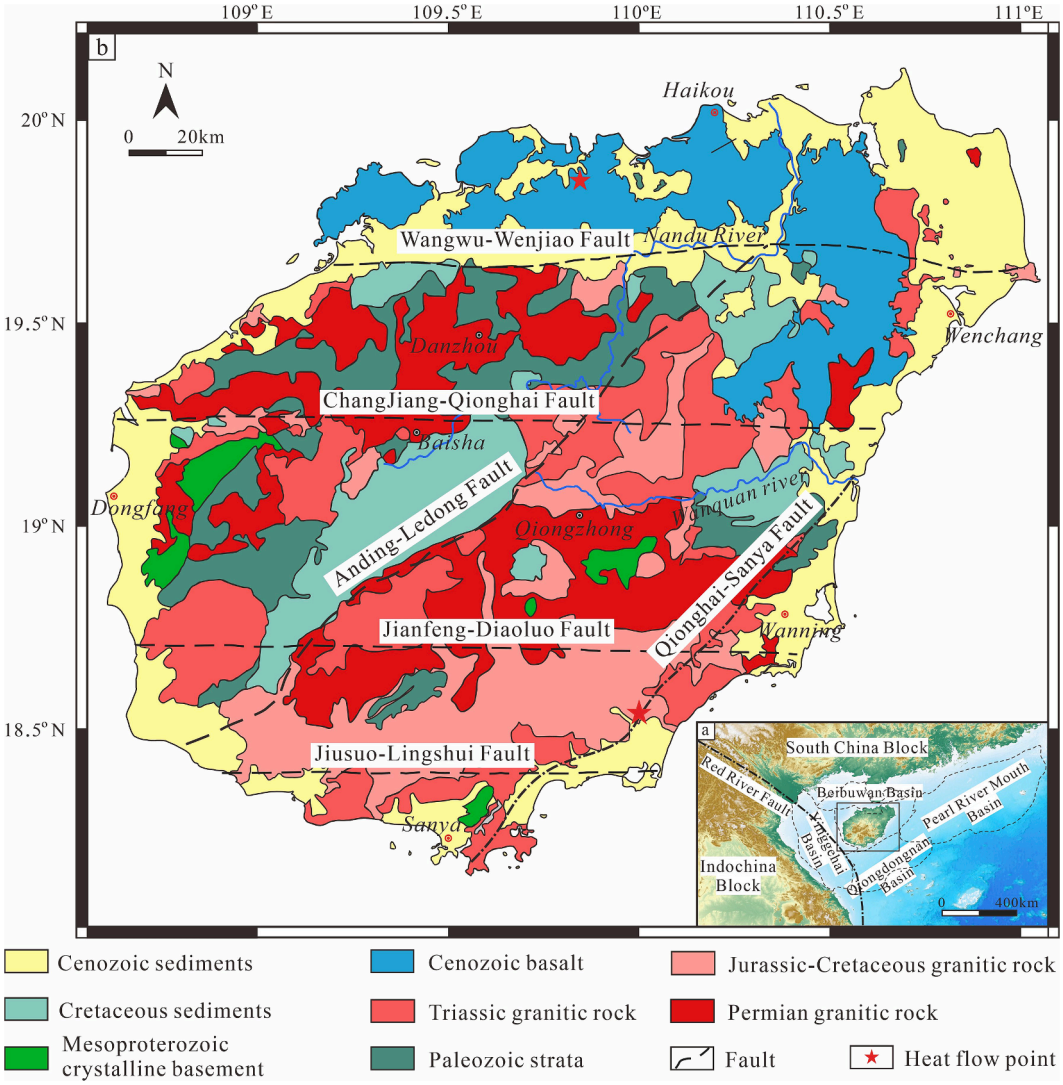

Fig. 1. Geological map of Hainan Island. (a) Structural location of Hainan Island; (b) Geological map of Hainan Island. The terrain contour data comes from ETOPO2022 data from the US Geophysical Center (NGDC).

3. Method and data

3.1. Calculation of lithosphere thermal structure

Establishing a crustal layering model is a crucial prerequisite for studying the temperature structure of the regional lithosphere, as variations in the model can significantly affect the final calculated temperature results. According to current research reports, information on the crustal structure of Hainan Island is limited, making it challenging to accurately model its crustal structure. Therefore, we have decided to integrate seismic wave velocities with the CRUST1.0 model to develop a crustal layering model for Hainan Island. Specifically, we use the CRUST1.0 model to delineate the thicknesses of both the sedimentary layer and the crust. Additionally, seismic wave velocities are employed to determine the thicknesses of the upper crust (Vp $<$ 6.2 km/s) and middle crust (6.2 km/s $\leq$ Vp $\leq$ 6.5 km/s). For seismic wave velocities, we adopt the three-dimensional seismic velocity model USTClitho2.0 of the Chinese continental crust and upper mantle, established by Han et al. (2022) using seismic wave velocity tomography techniques and simultaneously fitting body wave and surface wave dispersion data.

(1) Crustal temperature

Temperature in the deep crust is usually not directly measurable and is generally calculated by using the one-dimensional steady-state heat conduction equation. The equation is presented as follows:

$$T_Z = T_0 + qZ/K - (AZ^2)/2K \quad (1)$$

where T_z and T_0 are the temperatures at depth Z below the surface and at the top of the calculation segment, respectively (°C); q is the heat flow at the top of the calculation segment (mW/m^2); Z is the thickness of the calculation segment (km); K is the thermal conductivity of the rock within the calculation segment (W/(m·K)); A is the heat generation rate of the rock within the calculation segment (μW/m^3).

Considering that the thermal conductivity of rocks is influenced by temperature, this paper uses the formula $K = K_0(1 + cZ)(1 + b(T - 273.15))^{-1}$ for in-situ thermal conductivity correction, where b takes values of 1.5×10^{-3} K^{-1}、1.5×10^{-3} K^{-1}、0.8×10^{-4} K^{-1}and 1.5×10^{-4} K^{-1} respectively for the sedimentary layers, upper crust, middle crust and lower crust, c takes a value of 1.5×10^{-3} km^{-1}, and T represents the temperature (K) at a certain depth z (km). The initial values of thermal conductivity for the sedimentary layers, upper crust, middle crust, and lower crust are taken as 3.72 W/(m·K), 3.0 W/(m·K), 2.8 W/(m·K), and 2.6 W/(m·K), respectively, with the thermal conductivity of the sedimentary layer being the measured average value of samples. The thermal conductivity of the upper mantle is taken as 4 W/(m·K) and is not corrected for temperature.

The heat production rate for the sedimentary layer is determined based on the average value of samples, which is 1.39 μW/m^3 (Li et al., 2024). For the upper crust, a constant heat production rate of 1.25 μW/m^3 is adopted. For the middle and lower crusts, the heat production rates are calculated using the empirical formula proposed by Rybach and Buntebarth (1984), which correlates P-wave velocity with heat production rate: $\ln A = 12.6 - 2.17 \times v_p^0$. The heat production rate for the upper mantle is assumed to be a constant value of 0.03 μW/m^3. Table 1 summarizes the parameters for the crustal layering model.

There are significant differences in temperature and pressure conditions between in-situ seismic wave velocities and those measured under experimental conditions (293.15 K, 100 MPa). Therefore, it is essential to apply corrections to the in-situ seismic wave velocities. The correction formula was proposed by Rybach and Buntebarth (1984) as follows:

$$v_p^0 = v_p + (293.15 - T)\frac{\partial V_P}{\partial T} + (100 - P)\frac{\partial V_P}{\partial P} \quad (2)$$

where v_p represents the in-situ P-wave velocity. For the middle and lower crusts, the values of v_p are 0.0004 km/(s·K) and 0.0005 km/(s·K), respectively. The value of v_p for the upper crust is 0.0003 km/(s·K) (Wang, 2001).

Table 1
Model parameter.

Crustal stratification	Thickness (km)		Thermal conductivity (W/m·K)	Heat production rate (μW/m^3)
	Model	Plan	K_0	
Deposition layer	CRSUT 1.0	1.2 km	3.72	1.39
Upper crust	USTClitho 2.0	$V_p < 6.2$ km/s	3.00	1.25
Middle crust		6.2 km/s $\leq V_p \leq$ 6.5 km/s	2.80	1.26–2.17 × V_p
Lower crust		$V_p > 6.5$ km/s	2.60	1.26–2.17 × V_p

(2) Upper mantle temperature

Due to the lack of geothermal constraints on heat production rate and thermal conductivity in the deep upper mantle of the lithosphere, it is challenging to accurately estimate temperatures using one-dimensional thermal steady-state equations. Therefore, this study employs seismic S-wave velocity inversions to estimate temperatures at depths greater than 50 km. The seismic wave velocities are derived from the three-dimensional seismic velocity model USTClitho2.0 of the Chinese continental crust and upper mantle, established by Han et al. (2022).

The elastic modulus (μ) and density (ρ) of minerals at a certain depth in the upper mantle can be estimated based on measurements of elastic modulus and density obtained under ambient temperature and pressure conditions ($T_0 = 300$ K, $P_0 = 0$ GPa) in the laboratory. The estimation formula is as follows:

$$M(P,T,X) = M_0 + T_D\frac{\partial M}{\partial T} + (P - P_0)\frac{\partial M}{\partial P} + X\frac{\partial M}{\partial X} \quad (3)$$

$$\rho(P,T,X) = \rho_0\frac{\partial \rho}{\partial X}[1 - \alpha_0 - \alpha_1 T_D - \alpha_2 T_D^{-1} - \alpha_3 T_D^{-2} + \frac{P - P_0}{K}] \quad (4)$$

where $T_D = T - T_0$; X represents the iron content in the upper mantle (the value used in this study is 0.1); α is the rock thermal expansion coefficient, and other parameters are shown in Table 2.

The relationship between Vs wave velocity (Vs) and elastic modulus and density can be expressed as:

$$V_S(P,T) = \sqrt{\frac{\langle \mu \rangle}{\langle \rho \rangle}} \quad (5)$$

$$\langle \mu \rangle = \frac{1}{2}\sum_i (\lambda_i \mu_i + \frac{\mu_i}{\lambda_i}) \quad (6)$$

$$\langle \rho \rangle = \sum_i (\lambda_i \rho_i) \quad (7)$$

Table 2
Mineral elasticity parameters (Goes et al., 2000).

Parameter	Olivine	Orthopyroxene	Clinopyroxene	Garnet
ρ_0(g/cm^3)	3.222	3.198	3.280	3.565
$\partial\rho/\partial X$	1.182	0.804	0.377	0.758
μ_0(GPa)	82	81	67	92
$\partial\mu/\partial T$(MPa/K)	−14	−11	−10	−10
$\partial\mu/\partial P$	1.4	2.0	1.7	1.4
$\partial\mu/\partial X$	−30	−29	−6	7
$\alpha_0(10^{-5}\text{K}^{-1})$	2.010	3.871	3.206	0.991
$\alpha_1(10^{-8}\text{K}^{-2})$	1.390	0.446	0.811	1.165
$\alpha_2(10^{-2})$	0.1627	0.0343	0.1347	1.0624
α_3(K)	−0.3380	−1.7278	−1.8167	−2.5000

where ρ_i and μ_i represent the density and shear modulus of the ith mineral, respectively; ρ_i represents the proportion of the ith mineral.

Considering that Hainan Island has experienced frequent tectonic events during the Late Mesozoic to Cenozoic, this study adopts the proportions of upper mantle lithological components proposed by previous researchers, with approximately 68 % olivine, about 18 % orthopyroxene, approximately 11 % clinopyroxene, and about 3 % garnet (An and Shi, 2007; Shapiro and Ritzwoller, 2004; Zhang et al., 2018).

As depth increases, seismic wave velocities are influenced by anelasticity (Sobolev et al., 1996; Goes et al., 2000; Goes and Van, 2002). Anelastic correction is commonly applied using the anelastic factor Q, and the correction formula is as follows:

$$V_s(P,T,\omega) = V_s(P,T)\left[1 - \frac{Q^{-1}(\omega,T)}{2\tan(\pi a/2)}\right] \tag{8}$$

$$Q(\omega,T) = A\omega^a e^{(a\frac{H+PV}{RT})} \tag{9}$$

where Q represents the anelastic factor; A and a are anelastic constants, with values of 0.148 and 0.15 respectively; ω is the frequency; H is the activation energy, taken as 500 kJ/mol; V is the activation volume, taken as 20 cm^3/mol; and R is the universal gas constant.

The base of the thermal lithosphere corresponds to the boundary where the mode of heat transfer transitions from conductive above to convective below. The depth of the base of the thermal lithosphere generally corresponds to the mantle solidus temperature (at approximately 1300 °C). Given that the solidus is influenced by variations in mantle viscosity and mechanical properties (Pollack and Chapman, 1977; Cammarano et al., 2003; Deng and Tesauro, 2016), the presence of fluids in the upper mantle can lower the solidus temperature. Therefore, this study adopts a bottom temperature of 1250 °C for the thermal lithosphere.

3.2. Thermo-rheological structure calculation

The rheology of the lithosphere encompasses the deformation and flow processes of lithospheric materials under tectonic forces. The rheological structure of the lithosphere is primarily governed by its thermal conditions. Consequently, determining the thermal state of the lithosphere can provide deeper insights into its rheological behavior (Liu et al., 2003). The construction of the lithospheric rheological strength profile relies on quantitative calculations of rheological strength using experimentally derived constitutive equations, which describe both the brittle and ductile behaviors of the lithosphere.

The brittle strength of the lithosphere can be determined by the linear friction rupture formula (Sibson, 1974):

$$\sigma_b = \sigma_1 - \sigma_3 = (1-\lambda)\beta\rho g Z \tag{10}$$

where σ_b represents the yield limit of brittle deformation, MPa; λ is the pore fluid factor; β is the fault type parameter, which is taken as 1.2 in this paper (Ranalli and Murphy, 1987); ρ represents the medium density, kg/m^3; g is the acceleration of gravity, equal to 9.8 m/s^2.

Under conditions of high stress and temperature, rocks undergo creep deformation. In this case, the creep strength can be determined by the power-law creep equation (Kirby, 1983):

$$\sigma_d = \left(\frac{\varepsilon}{A}\right)^{\frac{1}{n}} e^{\left(\frac{H}{nRT}\right)} \tag{11}$$

where σ_d represents the yield limit of ductile deformation, MPa; ε is the strain rate, s^{-1}, which is taken as 10^{-14} s^{-1}; R is the gas constant, taken as 8.314 J/(mol·K); T is the temperature distribution within the lithosphere, K; A is the rheological parameter, $MPa^{-n}\cdot s^{-1}$; n is the stress exponent; and H is the activation enthalpy, J/mol. A, n, and H can all be determined through experiments.

The integrated lithospheric strength is obtained by vertically integrating the minimum yield strength (Hopper et al., 1993):

$$\sigma_y = \min(\sigma_b, \sigma_d) \tag{12}$$

$$S = \int_0^D \sigma_y(z)dz \tag{13}$$

where σ_y represents the yield strength of the lithosphere; S stands for the comprehensive lithospheric strength, MPa; D represents the lower boundary of the rheological lithosphere, km.

With changes in temperature, depth, and lithology, at a certain depth within the lithosphere, the brittle strength σ_b will be equal to the ductile strength σ_d.This depth is referred to as the brittle-ductile transition depth.

The lithosphere in Hainan Island is divided into five layers: sedimentary layer is represented by quartzite, the upper crust by granite, the middle crust by quartz diorite, the lower crust by diabase, and upper mantle of the lithosphere by peridotite. Rock mechanical parameters of each layer are provided in Table 3.

4. Result

4.1. Thermal structure of the lithosphere

With the continuous development of geothermics, different scholars have adopted various methods to classify the thermal structure of the lithosphere (Wang et al., 1996; Hu et al., 2001; Qiu et al., 2022). This study adopts the method defined by Qiu et al. (2022). According to this method, a crust (or mantle) heat flow of less than 25 mW/m^2 is considered “cold”, between 25 and 35 mW/m^2 is considered “warm”, and 35 mW/m^2 or above is considered “hot”.

Based on two measured heat flow values from the Fushan Depression and Lingshui areas in Hainan Island, combined with the established crustal layering model, we used the “backstripping method” (where D_i represents the thickness of the structural layer, km; A_i is the corresponding heat production rate of the structural layer, μW/m^3; q_s, q_m, and q_c represent the surface, mantel, and crust heat flows, mW/m^2, respectively) to calculate the crustal and mantle heat flows at the two measurement points in Hainan Island. The result (Fig. 2) shows that in the northern Fushan Depression, the crustal heat flow is 22 mW/m^2 and the mantle heat flow is 44 mW/m^2. The thermal structure of the lithosphere exhibits a “cold crust, hot mantle” pattern, with the mantle heat flow accounting for 67 % of the total heat flow. In the southern Lingshui region, the crustal heat flow is 24 mW/m^2 (Fig. 3), and the mantle heat flow is 49 mW/m^2. The thermal structure of the lithosphere also exhibits a “cold crust, hot mantle” pattern, with the mantle heat flow contribution rate consistent with that of the northern Fushan depression, accounting for 67 % of the total. The thermal structure types in the north

Table 3
Parameters of the lithospheric thermo-rheological structure.

Crustal layering	Representative lithology	Creep parameters A/ ($MPa^{-n}\cdot s^{-1}$)	n	Q/ (kJ/mol)	Density/ ($10^3 kg\cdot m^{-3}$)
Sedimentary Layer	Quartzite	6.7×10^{-6}	2.4	156	2.59
Upper crust	Granite	1.8×10^{-9}	3.2	123	2.61
Middle crust	Quartz diorite	1.3×10^{-3}	2.4	219	2.64
Lower crust	Diabase	2.0×10^{-4}	3.4	260	2.71
Upper mantle	Peridotite	1.9×10^{3}	3.0	420	3.30

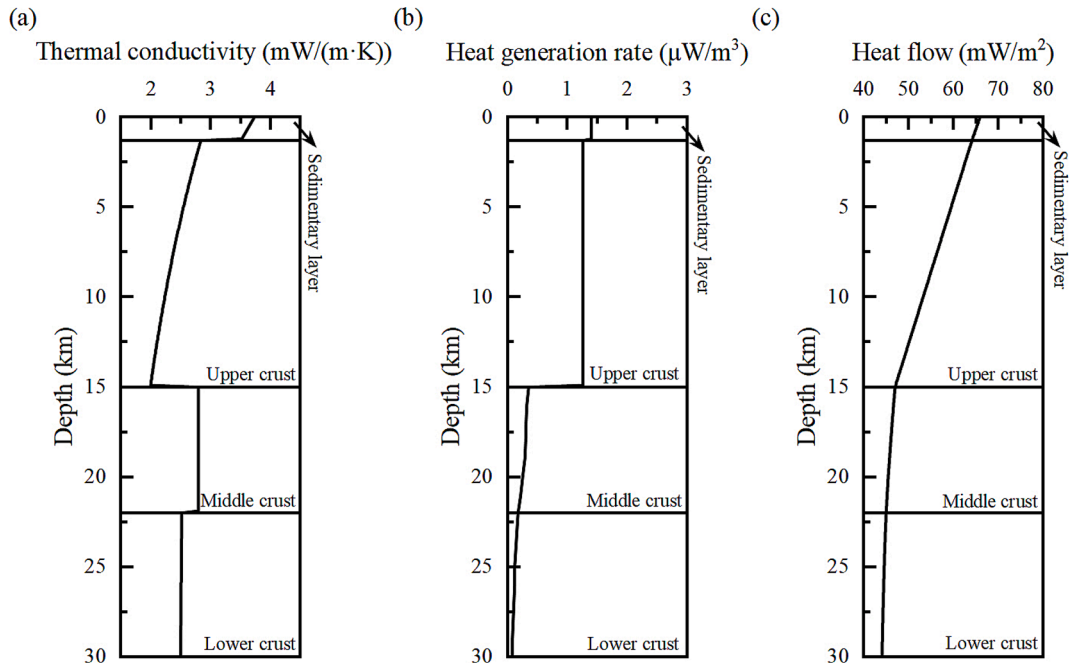

Fig. 2. Crustal structure models in the Fushan area of Hainan Island. (a) the changes in thermal conductivity; (b) the changes in heat generation rate; (c) the changes in heat flow of each layer of the crust.

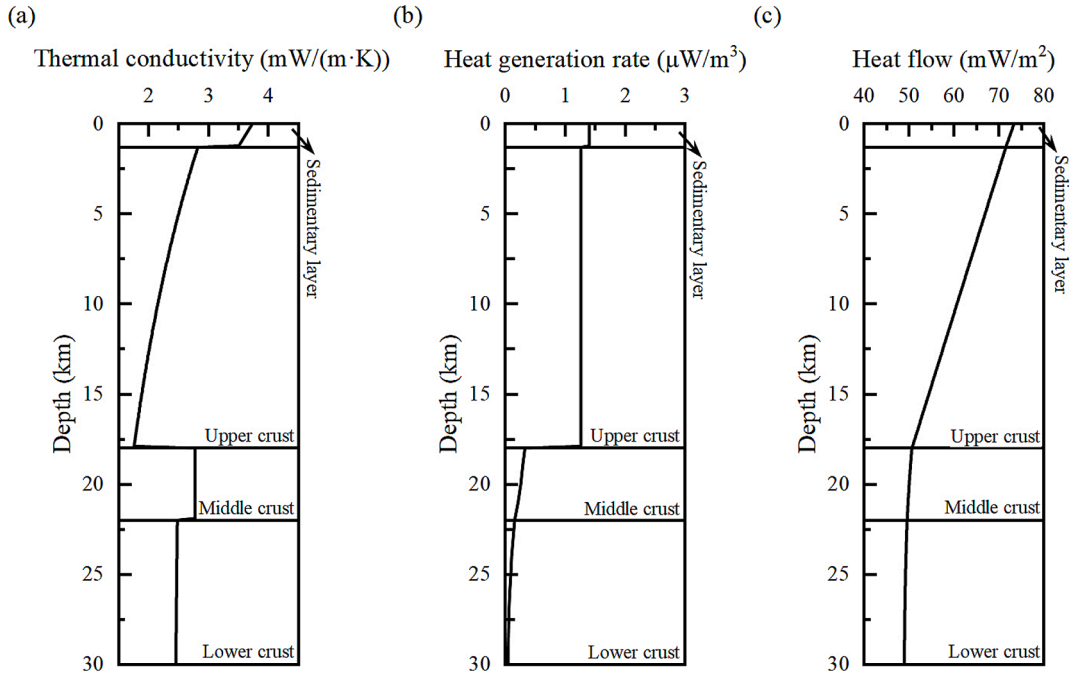

Fig. 3. Crustal structure models in the Lingshui area of Hainan Island. (a) the changes in thermal conductivity; (b) the changes in heat generation rate; (c) the changes in heat flow of each layer of the crust.

and south of Hainan Island are consistent, with the mantle contributing the majority of the surface heat flow, characterized by a "hot mantle" feature. This result is similar to the lithospheric thermal structure types observed in the four major basins surrounding Hainan Island (Beibu Gulf Basin, Yinggehai Basin, Qiongdongnan Basin, and Pearl River Mouth Basin) (Shan et al., 2011; Wu et al., 2022; Tang et al., 2011, 2014, 2018; He et al., 2000; Zhang et al., 2000). It indicates that the mantle heat is one of the important factors influencing the current geothermal field of Hainan Island and its surrounding areas.

The depth of the bottom boundary of the thermal lithosphere changes with the thermal uplift or subsidence of the upper mantle, which is an important basis for measuring the high-temperature thermal structure in the deep part. This paper calculates the thermal lithospheric thickness at two measured heat flow points using a joint method combining the one-dimensional thermal steady-state equation and seismic wave velocity inversion. The results indicate (Fig. 4) that the thickness of the thermal lithosphere in the Fushan Depression in northern Hainan is approximately 75 km, while in the Lingshui area in southern Hainan, it is about 150 km. Notably, the temperature below 100 km depth in the Lingshui region is nearly parallel to the mantle

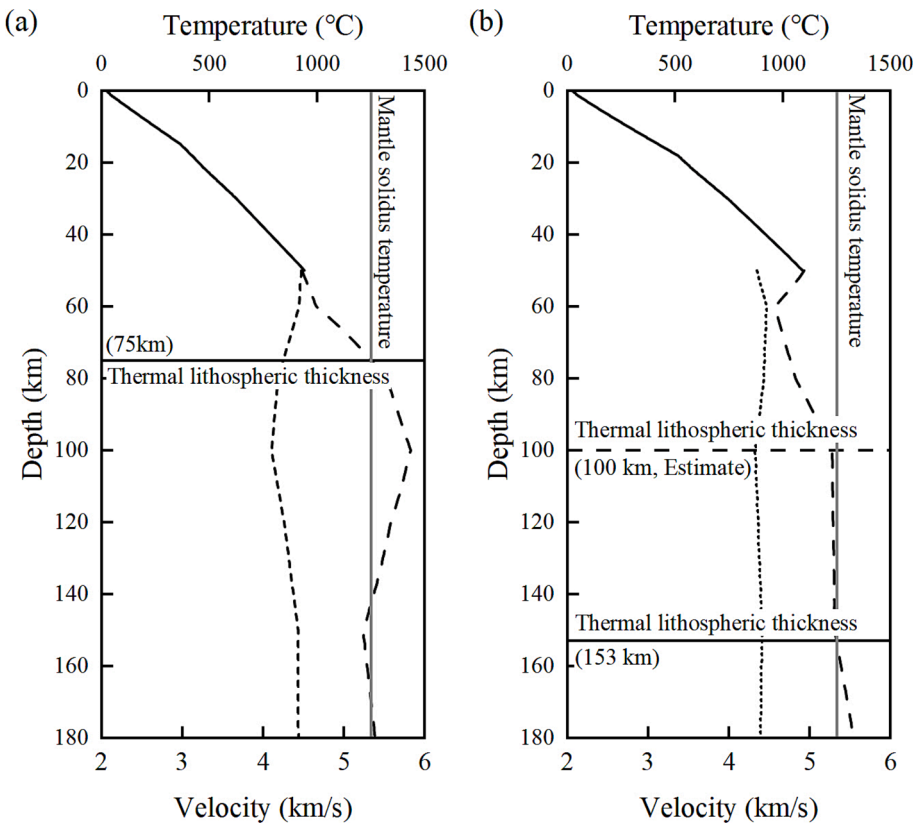

Fig. 4. Lithospheric temperature of the Fushan area (a) and Lingshui area (b) of Hainan Island. The straight line represents the thermal calculation result of the one-dimensional steady state heat conduction equation; The dashed line represents the thermal result of the Vs wave velocity inversion; Dotted line represents the Vs wave velocity.

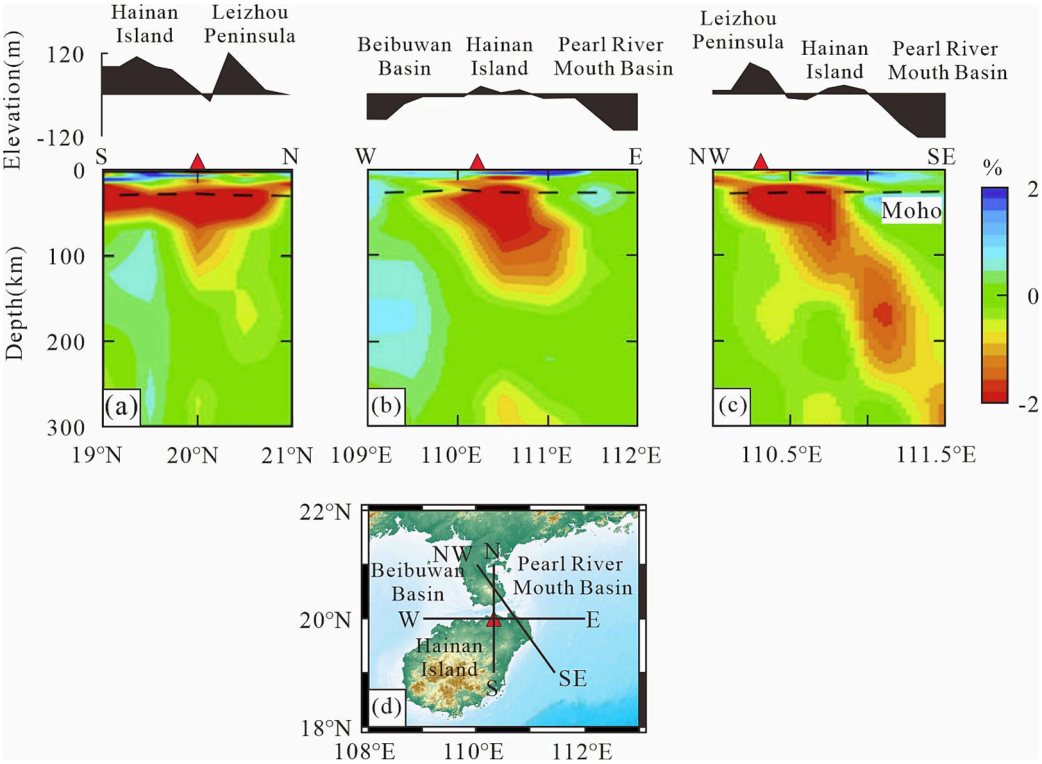

Fig. 5. Seismic velocity tomography image of Hainan Island and its surrounding areas (Lei et al., 2009).

solidus temperature of 1250 °C, exhibiting characteristics of convective heat transfer. Analysis suggests that the actual thickness of the thermal lithosphere in the southern Lingshui region should be less than 150 km, approximately 100 km.

The deep temperature in the northern Fushan area exhibits a phenomenon of "rapid increase followed by gradual decrease" (Fig. 4a). When the depth reaches approximately 100 km, the temperature begins to decrease and gradually falls below 1250 °C. As the depth reaches to ~ 150 km, the temperature begins to rise again. This depth range of temperature variation is correlated with a low-velocity zone for S-waves, suggesting a local abnormal high temperature extending from the bottom of the deep thermal lithosphere to 150 km in the Lingshui area. Additionally, the small-scale temperature anomaly is also observed at a depth of 50 km in the southern Lingshui region. The results of this calculation are highly similar to the high-resolution tomographic image of the upper mantle of Hainan Island determined by Lei et al. (2023) based on geophysical data of Hainan Island and its surrounding areas (Fig. 5). There is a widespread low-velocity anomaly in seismic wave velocities from the bottom of the crust to the deep upper mantle beneath Hainan Island, which corresponds to a high-temperature anomaly.

The temperature at a depth of 50 km obtained through S-wave velocity inversion aligns well with the estimation results from the one-dimensional thermal steady-state equation, demonstrating good consistency (Fig. 4). Based on the discovery, this study employs the temperature at a depth of 50 km obtained from Vs wave velocity inversion as the temperature constraint for the one-dimensional steady-state heat conduction equation at 50 km to perform inversion calculations for heat flow values within Hainan Island. To verify the accuracy and effectiveness of the inversion results, the study first conducted inversion calculations for two measured points before applying the method to the entire Hainan Island. The results show that the errors between the inversion outcomes and the measured values for the two measurement points are relatively small, indicating that the method can be used for estimating heat flow in the Hainan Island area (Table 4). Using the same spatial resolution (0.5° × 0.5°) as the seismic wave model USTClitho2.0, 15 points were selected across Hainan Island for heat flow inversion, with the results presented in the Table 4.

Fig. 6 presents the contour map of inverted surface heat flow. The results indicate that the surface heat flow of Hainan Island ranges from 61 to 77 mW/m^2, with an average value of 67 mW/m^2, significantly higher than the average heat flow of 62 mW/m^2 in Chinese mainland. The heat flow shows a clear distribution pattern of high in the south and low in the north, gradually decreasing from south to north. Figs. 7 to 10 show the curves of deep S-wave velocity and temperature variation at 15 selected locations in Hainan Island. The results reveal that the thermal lithosphere of Hainan Island is relatively thin overall, with the southern thermal lithosphere being thicker than that in the northern region. The variation curves of Vs wave velocity and temperature at 15 points are similar to those in the Fushan Depression and Lingshui area, indicating the presence of a low-velocity anomaly zone beneath the crust. This finding may suggest the existence of a high-temperature anomaly zone across the entire upper mantle of the Hainan Island lithosphere. The depth of the high temperature anomaly zone in the northern and central regions of Hainan Island is consistent with that of the Fushan Depression, ranging from 80 km to 150 km. The high-temperature anomaly zone in the southern region is relatively shallow, with a depth of approximately 40 km to 60 km.

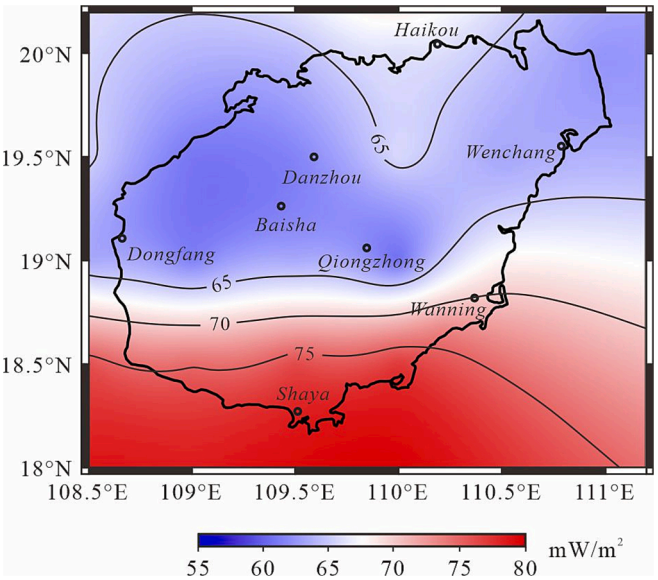

Fig. 6. Heat flow distribution map of Hainan Island.

4.2. Rheological strength

Fig. 11 shows the rheological structure profile of the lithosphere in the Fushan and Lingshui regions of Hainan Island. The results indicate that the rheological structure in the Fushan region exhibits two brittle layers and two ductile layers, forming a "brittle-ductile–brittle-ductile" structure. The entire sedimentary layer and most of the upper crust display brittle characteristics, while some strata in the upper part of the middle crust also display brittleness, with the remaining parts showing ductile features. There are two brittle-ductile transition zones in the region, located at depths of 11 km and 19 km, respectively (where the brittle layer transitions to the ductile layer is referred to as the brittle-ductile transition zone). In contrast, the rheological structure of the lithosphere in the Lingshui region shows significant differences. It is primarily characterized by ductile features, with brittleness only observed in the sedimentary layer and the upper part of the upper crust. The lower part of the upper crust and deeper levels are entirely ductile, forming a "brittle-ductile" structure. The brittle-ductile transition zone in this region is located at a depth of 10 km.

Table 4
Inverted values of heat flow in Hainan Island.

Number	Longitude	Latitude	Surface heat flow (mW/m^2)	Number	Longitude	Latitude	Surface heat flow (mW/m^2)
1	109.97	19.87	66* (65)	10	109.50	19.50	62
2	110.22	18.68	73* (74)	11	110.00	19.50	66
3	109.00	18.50	75	12	110.50	19.50	63
4	109.50	18.50	76	13	111.00	19.50	64
5	110.00	18.50	77	14	109.50	20.00	64
6	109.00	19.00	61	15	110.00	20.00	66
7	109.50	19.00	63	16	110.50	20.00	65
8	110.00	19.00	61	17	111.00	20.00	62
9	110.50	19.00	68				

Note: *represents the measured heat flow value (Hu et al., 2001). The parentheses represents the inverted heat flow value. For example, 66*(65)indicates that the measured value is 66 mW/m^2. 65 mW/m^2, is the inverted heat flow value.

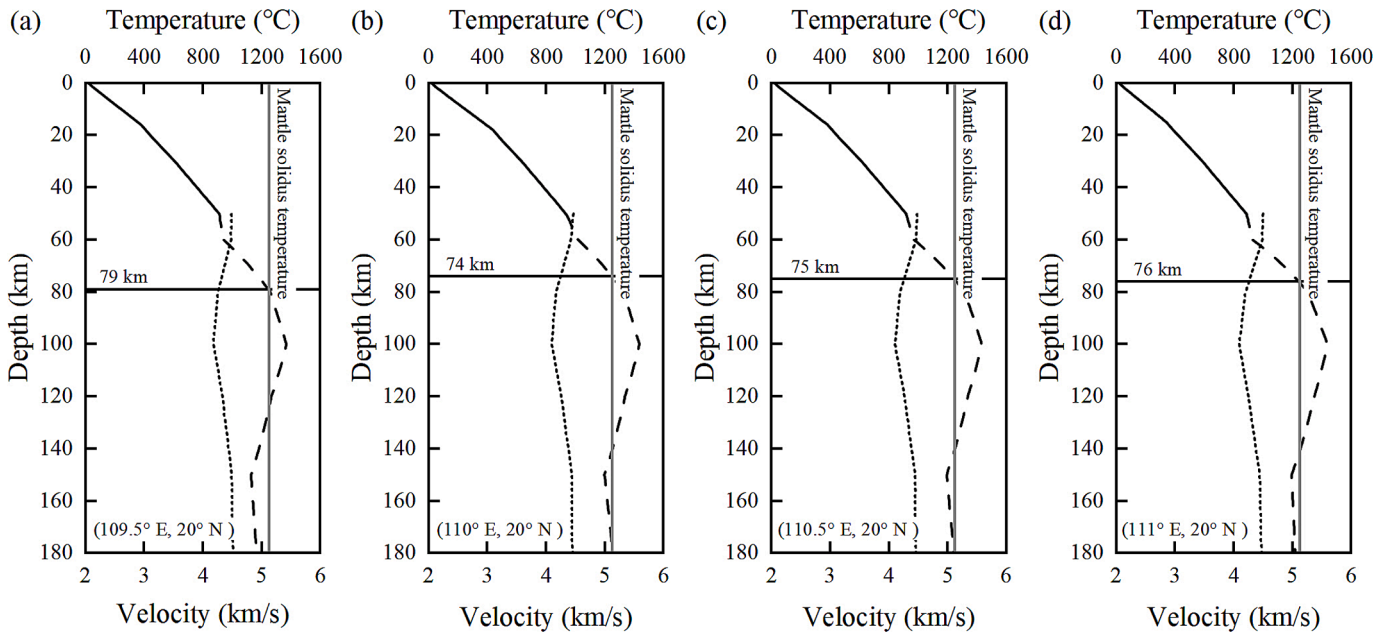

Fig. 7. Temperature of the lithosphere at various points of 20°N in Hainan Island.

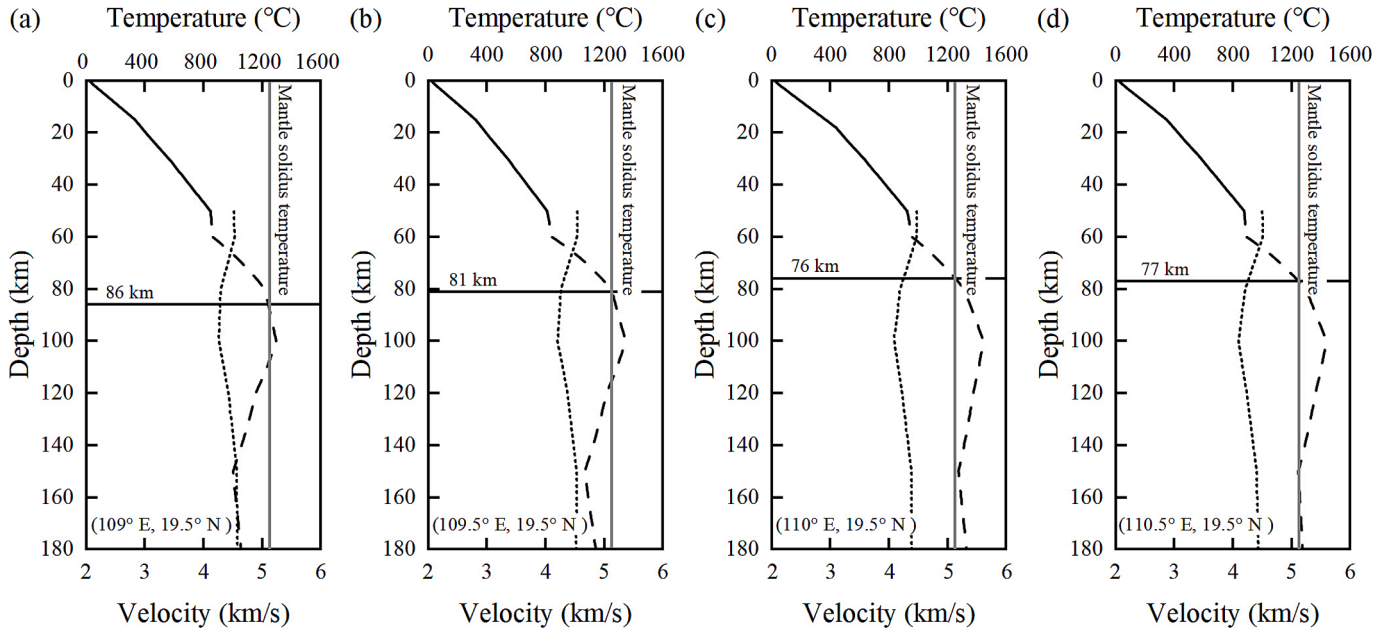

Fig. 8. Temperature of the lithosphere at various points of 19.5°N in Hainan Island.

Not only do the rheological structures of the northern and southern regions of Hainan Island show significant differences, but there are also large discrepancies in their rheological strengths. The total lithospheric strength in the Fushan Depression in the north is approximately 6×10^{12} Pa·m ~ 7×10^{12} Pa·m, with the crust contributing about 73 % of the total strength. In contrast, the total lithospheric strength in the Lingshui region in the south is only 2×10^{12} Pa·m ~ 3×10^{12} Pa·m, with the crust providing almost all of the lithospheric strength, accounting for approximately 88 %.

Based on temperature curves from 17 points, we calculated the lithospheric strength at each point and subsequently created a contour map (Fig. 12). The results indicate that the distribution of total lithospheric strength in Hainan Island is inversely correlated with the distribution of heat flow. In areas with high heat flow values, the total lithospheric strength is relatively low, while in areas with low heat flow values, the total strength is relatively high. The distribution characteristics of lithospheric strength are mainly characterized by high in the north and low in the south, with a total strength range of 1×10^{12} Pa·m ~ 20×10^{12} Pa·m. We further presented a map showing the distribution of crustal strength contribution on Hainan Island (Fig. 7), revealing that the crust contributes more than 50 % of the total lithospheric strength across the island. In the southern region, crustal strength contributes the most, almost completely determining the total strength of the lithosphere in the area, with a contribution rate of over 90 %. In the central region of Hainan Island, the crust contributes the least to the overall strength of the lithosphere. Overall, Hainan Island exhibits typical rheological characteristics of “strong crust, weak mantle”.

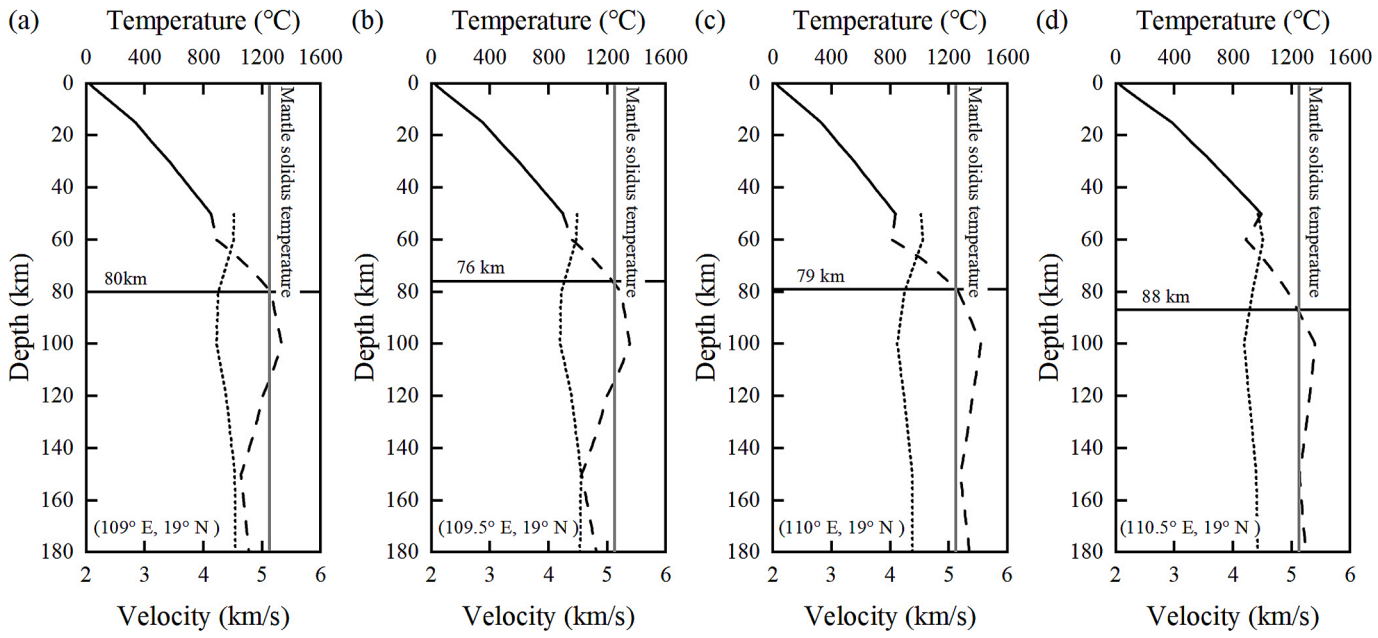

Fig. 9. Temperature of the lithosphere at various points of 19°N in Hainan Island.

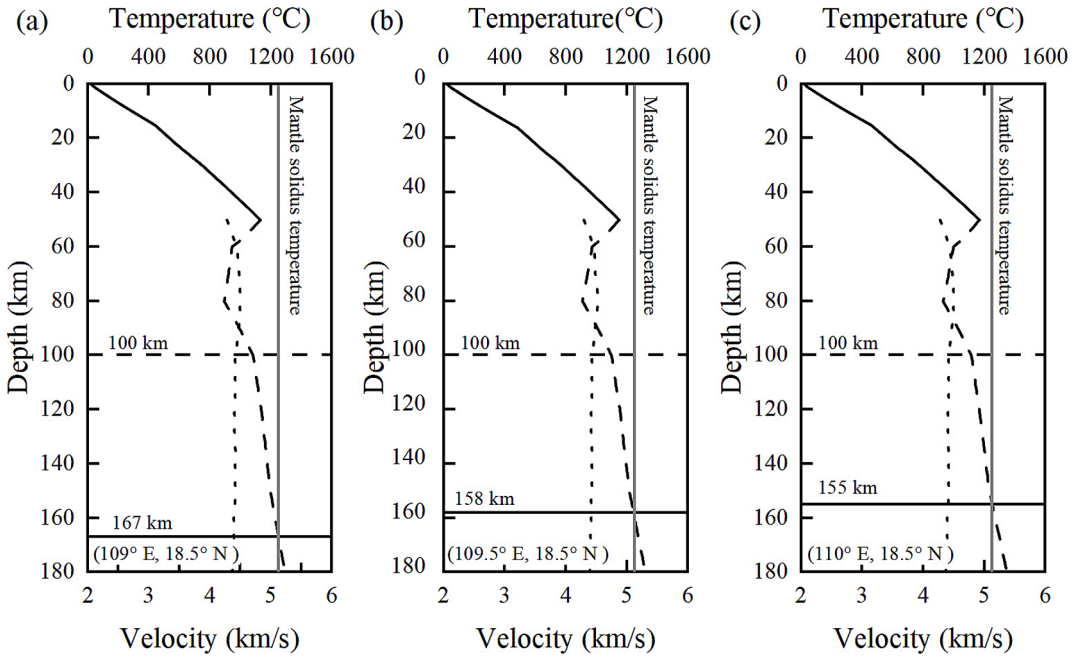

Fig. 10. Temperature of the lithosphere at various points of 18.5°N in Hainan Island.

5. Discussion

5.1. Formation of high temperature anomaly zone

Based on the temperature variation curves derived from two measured heat flow points and 15 inversion points (Fig. 4 and Fig. 7 ~ 10), the thickness of the thermal lithosphere in Hainan Island is relatively thin, ranging approximately from 70 to 100 km. We have identified a distinct high-temperature anomaly zone in the upper mantle, which also appears as a low-velocity zone on S-waves velocity. This anomaly zone extends from depths of 80 to 150 km in the central and northern regions, whereas in the south, it shifts upwards to a depth of 40 to 60 km. This finding suggests the potential existence of large-scale molten magma beneath Hainan Island.

Previous studies have revealed the presence of a mantle plume extending from the top of the upper mantle to the deep within the mantle beneath the South China Sea (Huang et al., 2012; Huang et al., 2015; Chen, 2021), which is academically known as the Hainan mantle plume. The upwelling pattern of the Hainan plume has two important characteristics (Fig. 13). Firstly, the Hainan mantle plume presents a continuous, mushroom-shaped low-speed anomaly that extends all the way to the lower mantle, featuring a tilted tail and a large, asymmetric crown. Secondly, the low-velocity anomaly of the Hainan mantle plume varies with depth, demonstrating obvious layering characteristics (Xia et al., 2016). We believe that the high-temperature anomaly zone identified in this study may be a consequence of the upwelling of the

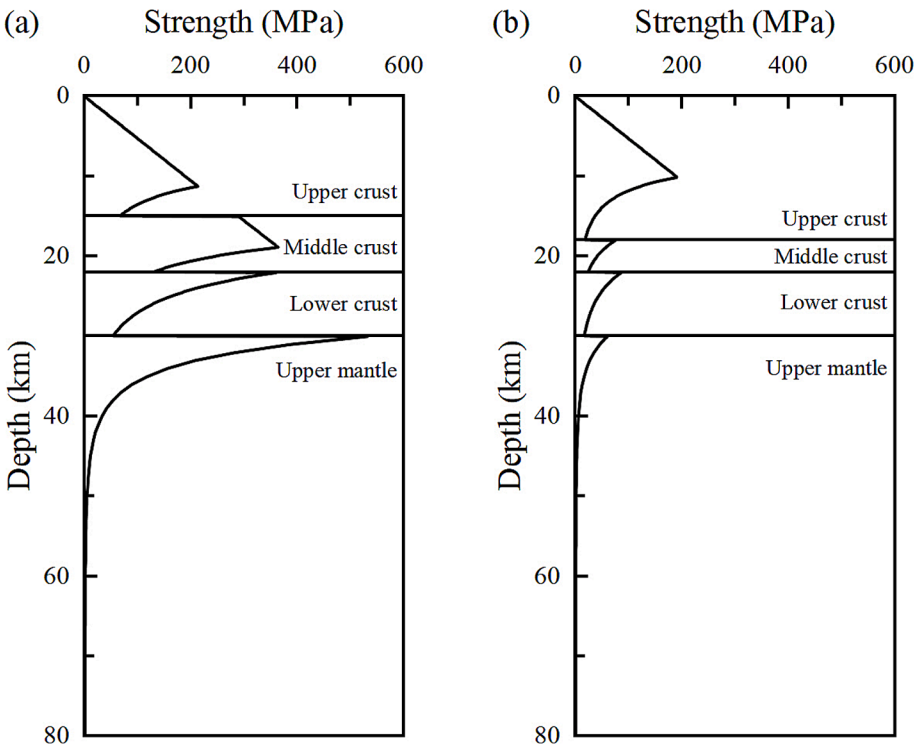

Fig. 11. Rheological structure of Fushan area (a) and Lingshui area (b) in Hainan Island.

Hainan mantle plume.

5.2. Mechanism of differences in thermo-rheological structure of the lithosphere

The heat flow in Hainan Island increases progressively from north to south, accompanied by a similar trend in the thickness of the thermal lithosphere. This phenomenon contradicts the conventional expectation that high heat flow corresponds to a thinner lithosphere. Estimates based on the one-dimensional steady-state heat conduction equation indicate that the thermal lithosphere thickness is approximately 71 km in the north and 61 km in the south, aligning with the general pattern. However, seismic wave inversions yield different results, showing the southern thermal lithosphere reaching up to 100 km in thickness, while the northern thickness remains relatively consistent with estimates derived from the one-dimensional steady-state heat conduction equation, at around 75 km. Our analysis suggests that this discrepancy may be closely related to thermal disturbances caused by mantle plume upwelling. Mantle plume upwelling not only provides additional heat but also induces local thermal convection, leading to complex thermal structures. Consequently, under the influence of mantle plume activity, the one-dimensional steady-state heat conduction equation fails to accurately reflect the true thickness of the lithosphere. Additionally, Gao et al. (2020) estimated the lithosphere thickness of Hainan Island to be approximately 70 ~ 80 km based on geological and geophysical data. Combining the results from both models and previous studies, we infer that the thickness of the thermal lithosphere in Hainan Island ranges from 71 to 75 km in the north and fluctuates between 61 and 80 km in the south. The significant variation in the southern thermal lithosphere thickness is likely due to intense thermal disturbances caused by mantle plume upwelling, which complicates the changes in thermal lithosphere thickness and may result in a thicker thermal lithosphere in high heat flow areas compared to low heat flow areas.

The variations in the thermo-rheological structural characteristics of Hainan Island's lithosphere are also reflected in the lithospheric strength profiles. The distribution of total lithospheric strength in Hainan Island is significantly negatively correlated with the heat flow distribution within the island. Areas with lower surface heat flow exhibit greater lithospheric strength, while areas with higher surface heat flow show reduced strength. Increased heat flow leads to heating and softening of the lithosphere, thereby reducing its overall strength. The dominant source of lithospheric strength gradually shifts from the upper mantle to the upper crust (Liu et al., 2003). Consequently, heat flow magnitude is one of the primary factors controlling lithospheric strength and serves as a direct indicator of the total lithospheric strength.

In addition, previous studies have suggested that factors affecting the rheological strength of the lithosphere include crustal thickness and lithospheric material composition (Ranalli et al., 1995; Lavier and Steckler, 1997; Liu et al., 2003). Compared to rocks in the deep crust and upper mantle, sediments exhibit lower thermal conductivity, leading to slower heat dissipation and accumulation of higher temperatures. This results in softening of the lower crustal material and ultimately reduces the strength of the lithosphere (Lavier and Steckler, 1997).

5.3. Seismic activity controlled by thermo-rheological structures

Continental earthquakes predominantly occur within the crust, with almost no earthquakes occurring within the mantle (except for deep mantle earthquakes related to subduction), and are mainly concentrated in the brittle layers of the crust. Xie et al. (2006) studied the characteristics of seismic activity on Hainan Island and found that the focal depths of crustal earthquakes in the Leiqiong Fault Depression (located in northern Hainan Island) are primarily shallower than 19 km. Xu et al. (2014) used the double-difference seismic relocation method to reposition earthquakes that occurred in Hainan Island between 2000 and 2012. Their results indicated that the depth range of earthquake sources in Hainan Island was primarily below 20 km, with the vast majority located at approximately 10 km. These findings are largely consistent with the brittle-ductile transition depth calculated in this study. The relationship between the brittle-ductile transition depth and the maximum focal depth of earthquakes can serve as an indicator of the maximum focal depth in a region, suggesting that the thermo-

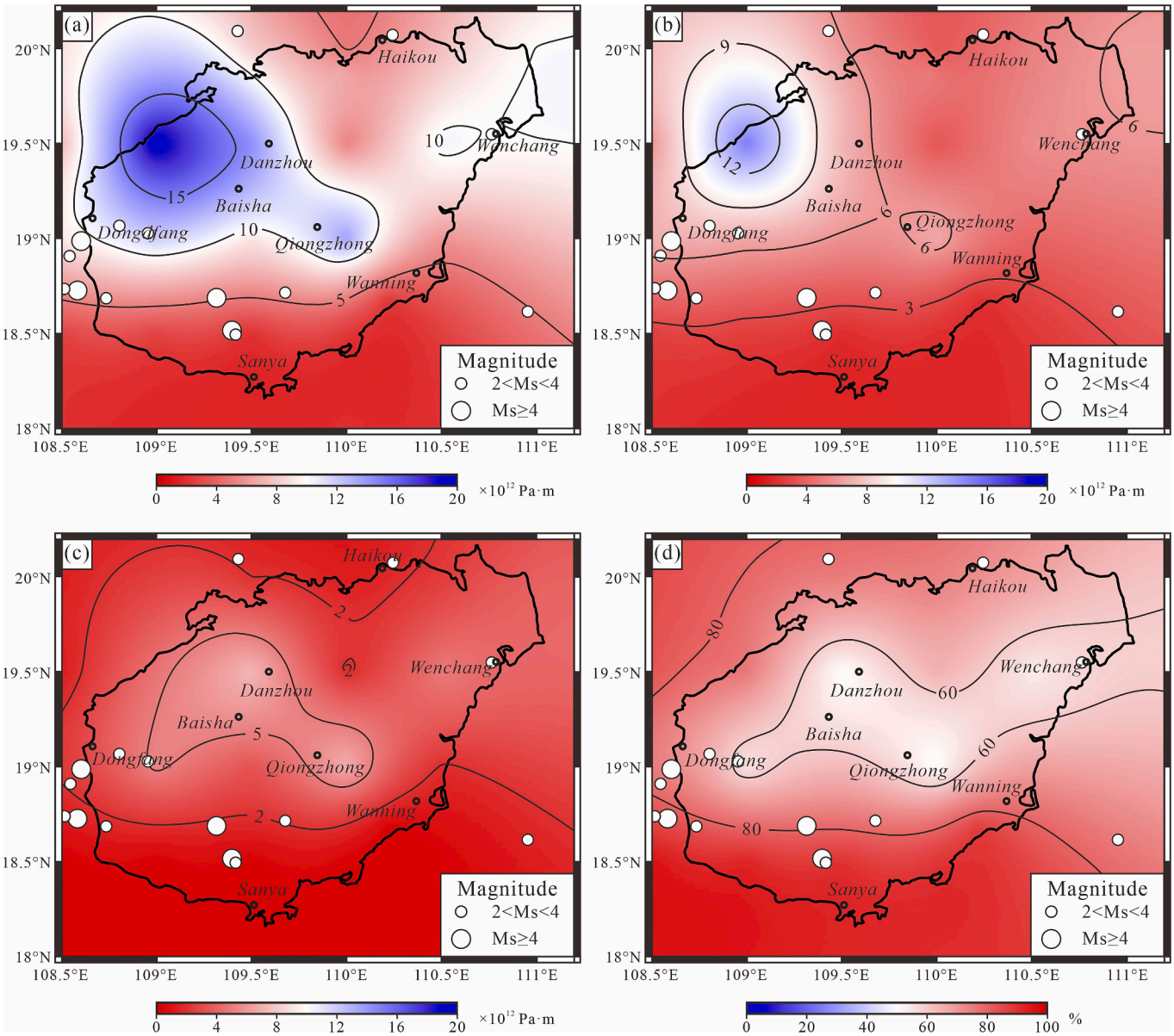

Fig. 12. Distribution of lithospheric strength in Hainan Island. (a) Distribution of total strength of the lithosphere; (b) Crustal strength; (c) Mantle strength; (d) The percentage of crustal strength to total strength.

rheological structure can influence regional seismic activity to some extent. Furthermore, earthquakes are prone to occur in areas with weak rheological strength (Fig. 7). Consequently, it is evident that the thermo-rheological strength of the lithosphere plays a significant role in controlling seismic activity in seismically active zones.

5.4. *The dynamic process of high heat flow formation in Hainan Island*

The lithosphere of Hainan Island exhibits a "cold crust, hot mantle" thermal structure, with the mantle contributing over 65 % of the heat flow. This thermal structure is similar to that observed in the surrounding four major basins: the Beibu Gulf Basin, the Yinggehai Basin, the Qiongdongnan Basin, and the Pearl River Mouth Basin (Shan et al., 2011; Wu et al., 2022; Tang et al., 2011, 2014, 2018; He et al., 2000; Zhang et al., 2000). The "heat"-dominated mantle structure suggests that the thermal state of the lithosphere in Hainan Island and its surrounding areas may be controlled by the same dynamic processes. Additionally, Hainan Island also displays characteristics of thin lithospheric thickness and a "weak mantle", collectively indicating a relatively soft and hot lithosphere.

The formation of a soft and hot lithosphere is typically closely related to dynamic processes within the region. For example, in the coastal regions of eastern China, the subduction of the Pacific Plate triggers the upwelling of hot and wet asthenospheric materials from the mantle transition zone, leading to the development of a soft and hot lithosphere (Dong et al., 2022; He, 2014; Jia et al., 2022; Liang et al., 2022; Yang and Liu, 2024; Zhang et al., 2019). In the Hainan Island region, under the combined influence of the Hainan mantle plume upwelling and the subduction of the Pacific Plate beneath the Eurasian Plate, similar changes may occur in the lithosphere. These two dynamic processes result in altered temperature conditions in the deep lithosphere, dehydration of deep-seated materials, and accompanying mantle material upwelling. During this process, a significant amount of heat from the deep mantle is transported to the upper part of the lithospheric mantle, causing the lithosphere to be heated and thinned, leading to large-scale thermal disturbances in the region. Ultimately, this manifests at the surface as high surface heat flow and active magmatic activity.

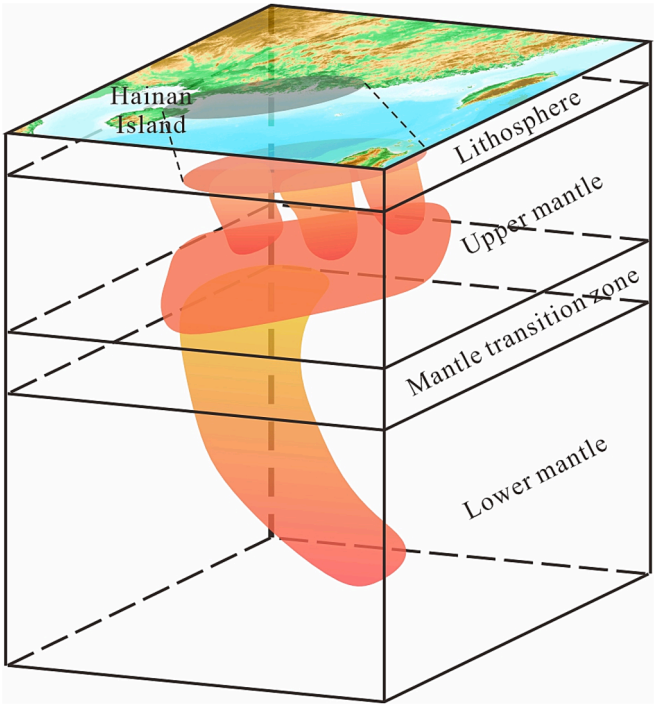

Fig. 13. Hainan mantle plume upwelling (Chen, 2021).

5.5. Enrichment mechanism of geothermal resources in Hainan Island

In recent years, significant breakthroughs in geothermal exploration on Hainan Island have been achieved, with multiple deep wells successfully revealing abundant high-temperature geothermal resources. In northern Hainan Island, the Haikou dry hot rock well reached a temperature of 156 °C at a depth of 4387 m. The overlying layers of low thermal conductivity basalt (thermal conductivity of 1.52 W/(m·K)) and clastic rocks (thermal conductivity of 2.53 W/(m·K)) act as insulating layers, effectively maintaining the high temperature of the thermal reservoir (Li et al., 2024). Meanwhile, Fushan deep geothermal well 1 (Fushen Re1) reached a high temperature of 188.71 °C at a depth of 5223 m and encountered a weathered granite crust at a depth of over 4000 m (Luo et al., 2024; Qian et al., 2024). The high heat production rate of the granite (3.28 μW/m^3) generates substantial heat within the formation, combined with the insulating effect of the overlying low thermal conductivity sedimentary layers, resulting in such high temperatures in a low heat flow area (Li et al., 2024). Combining the exploration results from these two wells, it is evident that the geothermal resources in northern Hainan Island primarily originate from deep weathered granite crust layers and anomalous heat sources, with low thermal conductivity cap rocks enhancing the insulating effect of the formations, thereby creating favorable conditions for thermal reservoirs in the northern region. In contrast, the geothermal genesis in southern Hainan Island differs markedly. Due to the absence of low thermal conductivity cap rocks, the heat preservation efficiency in most areas of the south is limited. However, the widespread distribution of thick, high heat production granite layers (up to 8 km in thickness) in this region provides sufficient heat replenishment due to their high heat production rate, effectively compensating for the heat loss caused by the lack of cap rocks (Zhang et al., 2015). Additionally, the presence of deep magma chambers contributes additional heat sources to shallow geothermal resources. Therefore, despite the lack of effective thermal reservoir cap rocks in southern areas, the thick granite layers render some southern regions still possessing good potential for geothermal reservoirs, warranting further exploration and development.

6. Uncertainty and sensitivity analysis

By employing both the heat conduction equation and seismic wave inversion methods, we have developed a thermal model of the lithosphere in Hainan Island, China. Using the temperature data from this model, combined with rheological parameters, we conducted simulations to calculate the rheological strength of Hainan Island. However, it is important to acknowledge that the computational process inherently involves limitations and uncertainties (Table 5 and Fig. 14).

Hainan Island is situated in a tectonically active region, where the deep temperature cannot be effectively estimated using the steady-state heat conduction equation (Jaupart et al., 2007). Therefore, we utilized seismic wave velocities to invert temperatures below 50 km. However, the presence of partial melting or fluids in the upper mantle can introduce uncertainty into seismic wave velocities. Based on the thermal structure model established in this study, we investigated the temperature variations resulting from different levels of uncertainty in seismic wave velocities. When the uncertainty is 1 %, at a depth of 50 km, the inverted temperature deviates by approximately 60 to 70 °C (−9% to + 7 %) from the normal value. At 150 km, the temperature difference is about 70 °C (−5% to + 5 %). When the uncertainty increases to 5 %, there is a significant deviation of 270 to 450 °C (−48 % to + 29 %) at 50 km, and the temperature difference at 150 km is approximately 250 to 380 °C (−31 % to + 20 %). When calculating heat flow values using temperature data inverted from seismic waves, a 1 % uncertainty leads to a deviation of 4 % to 6 %, while a 5 % uncertainty results in a substantial deviation of 17 % to 33 %. Detailed data on these differences and temperature variations are presented in Table 5 and Fig. 14. The anelastic parameters can also increase the uncertainty in temperature estimation, but they significantly impact the results only at high temperatures (above 1500 °C). In moderate to low-temperature environments (below 1300 °C), the introduced uncertainty is negligible (Dong et al., 2022). Notably, variations in mantle composition have minimal influence on the inverted temperature structure (Nolet and Zielhuis, 1994; Sobolev, 1996; Goes, 2000). Furthermore, the selection of thermophysical parameters greatly affects the calculation of crustal temperature, which in turn impacts the results of lithospheric thermal thickness and lithospheric strength (Table 5) (Yang et al., 2023).

7. Conclusions

Using geothermal data and thermophysical properties of rocks, in conjunction with geophysical and petrological data, we have inferred the thermo-rheological structure of the lithosphere beneath Hainan Island, China. The key findings can be summarized as follows:

(1) The thermal structure of the lithosphere beneath Hainan Island is characterized by “cold crust, hot mantle”, with the mantle heat flow contributing over 65 % of the total heat flow, due to the relatively thin thermal lithosphere.

(2) A high-temperature anomaly zone exists in the upper mantle beneath Hainan Island, potentially associated with the upwelling of the Hainan mantle plume.

(3) The current high heat flow and thin thermal lithosphere thickness on Hainan Island are influenced by the upwelling of the Hainan mantle plume and the subduction of the Pacific Plate.

(4) The rheological strength of the lithosphere is significantly affected by terrestrial heat flow. Increased heat flow leads to higher deep temperatures and reduced lithospheric strength, making the lithosphere softer. Regional heat flow values provide a reliable indicator of the lithosphere’s rheological strength. “Heat” plays a crucial role in determining the rheological properties of the lithosphere.

CRediT authorship contribution statement

Kefu Li: Writing – review & editing, Writing – original draft, Visualization, Methodology, Investigation, Data curation,

Table 5
Impact of Vs wave velocity uncertainty on simulation results.

Uncertainty	Temperature (℃) 50 km	100 km	Thermal lithospheric thickness (km)	Surface heat flow (mW/m^2)	Lithospheric strength ($\times 10^{12}$ Pa·m)
0 (Actual)	928	1212	75	65.8	6.7
0 (Inversion)	928	1212	75	65.2 (−1%)	7.2 (+7%)
+1%	855 (−9%)	1151 (−5%)	78 (+4%)	61.8 (−6%)	11.4 (+70 %)
+5%	481 (−48 %)	832 (−31 %)	99 (+32 %)	44.0 (–33 %)	59.6 (+790 %)
−1%	993 (+7%)	1269 (5 %)	72 (−4%)	68.3 (+4%)	4.9 (+27 %)
−5%	1193 (+29 %)	1454 (+20 %)	61 (−19 %)	78.1 (+17 %)	2.0^2 (+70 %)

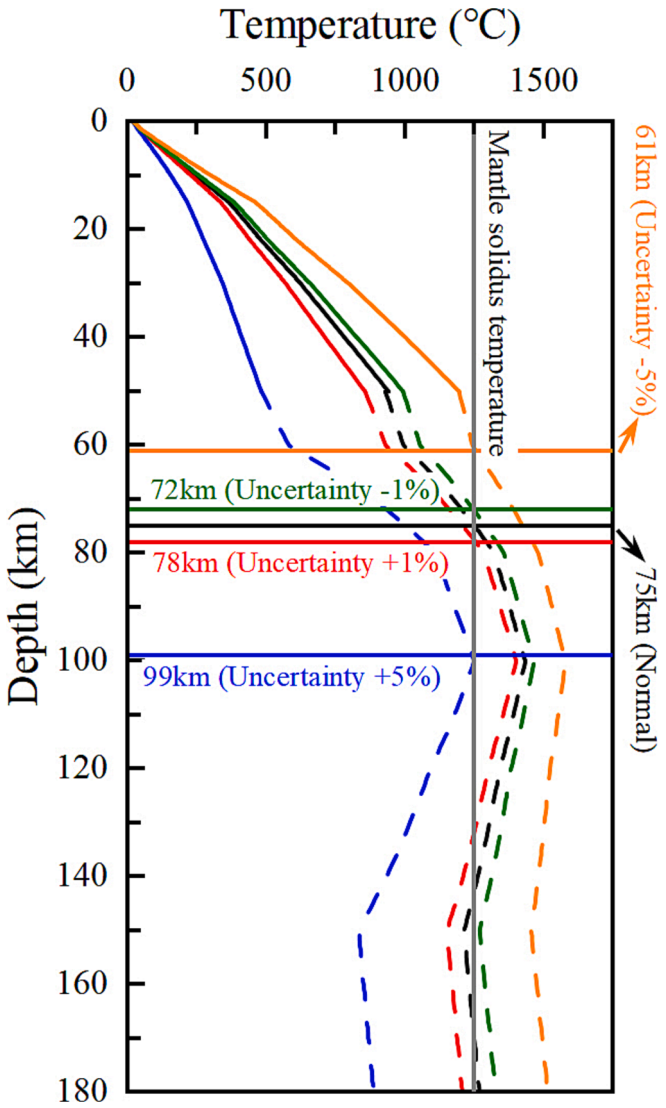

Fig. 14. Impact of Vs wave velocity uncertainly on temperature. In the temperature curves, the solid line represents the calculation results from the steady-state conduction equation. The dashed line represents the results from seismic wave velocity inversion. The black curve represents the temperature curve for the Lingshui area. The red curve represents the temperature result obtained through inversion when the seismic wave uncertainty is increased by + 1 %. The green curve represents the temperature result with a −1% uncertainty. The blue curve represents the temperature result with a + 5 %. The orange curve represents the temperature result with a −5% uncertainty.

Conceptualization. **Chuanqing Zhu:** Writing – review & editing, Supervision, Project administration, Methodology, Funding acquisition, Conceptualization. **Mengfei Zhang:** Writing – review & editing, Visualization. **Shudi Xing:** Writing – review & editing, Visualization, Investigation. **Yanyu Jia:** Writing – review & editing. **Chenxing Li:** Writing – review & editing.

Declaration of competing interest

The authors declare that they have no known competing financial interests or personal relationships that could have appeared to influence the work reported in this paper.

Acknowledgements

This study is supported by the National Key Research and Development Program of China (2021YFA0716003).

Data availability

Data will be made available on request.

References

An, M.J., Shi, Y.L., 2007. Three-dimensional temperature field of crust and upper mantle in China continental. Science in China Series D: Earth Sciences 37 (6), 736–745.
Cammarano, F., Goes, S., Vacher, P., et al., 2003. Inferring upper-mantle temperatures from seismic velocities. Physics of the Earth Planetary Interiors 138 (3), 197–222.
Chao, H.X., Han, X.H., Yang, Z.H., et al., 2016. New exploration of geotectonic characteristics of Hainan Island. Earth Science Frontiers 23 (4), 200–211.
Chen, M.X., Xia, S.G., Yang, S.Z., 1991. Local geothermal anomalies and their formation mechanisms on Leizhou Peninsula. South China. Chinese Journal of Geology 4, 369–383.
Chen, Y.M., 2008. Current Status of Geothermal Resources on Hainan Island and Suggestions for Exploration, Development, and Utilization. Scientific and Technological Management of Land and Resources 25 (06), 61–65.
Chen, Y.P., 2021. Hainan mantle plume from P wave finite frequency tomography. Harbin Institute of Technology, Harbin.
Deng, Y., Tesauro, M., 2016. Lithospheric strength variations in Mainland China: Tectonic implications. Tectonics 35 (10), 2313–2333.
Dong, Y., You, T., Dapeng, Z., et al., 2022. Thermal and rheological structure of lithosphere beneath Northeast China. Tectonophysics 840, 229560.
Gao, F.L., Yang, X.Q., Wu, G.A., et al., 2009. Characteristics of Hot Springs and Genesis of Geothermal Water on Hainan Island. Journal of Jilin University: Earth Science Edition 39 (2), 281–287.
Gao, W., Guo, Z.H., Zhou, J.X., et al., 2020. High-Precision Aeromagnetic Characteristics and Curie Isotherm Depth Analysis of Hainan Island. Acta Geologic Sinica 94 (11), 3249–3262.
Goes, S., Govers, R., Vacher, P., 2000. Shallow mantle temperatures under Europe from P and S wave tomography. Journal of Geophysical Research Solid Earth 105 (B5), 11153–11169.
Goes, S., Van Der Lee, S., 2002. Thermal structure of the North American uppermost mantle inferred from seismic tomography. Journal of Geophysical Research Solid Earth 107 (B3), 2050.
Han, S.C., Zhang, H.J., Xin, H.L., et al., 2022. Updated Unified Seismic Tomography Models for Continental China Lithosphere from Joint Inversion of Body-Wave Arrival Times and Surface-Wave Dispersion Data. Seismological Research Letters 93 (1), 201–215.
He, L.J., Hu, S.B., Wang, J.Y., 2001. Characteristics of thermal structure of lithosphere in eastern segment China mainland. Progress in Natural Science (in Chinese). 11 (9), 966–969.
He, L.J., Xiong, L.P., Wang, J.Y., et al., 2000. Simulation of Tectonic and thermal evolution in the Yinggehai Basin. Science in China Series D: Earth Sciences 30 (4), 415–419.
He, L.J., 2014. The rheological boundary layer and its implications for the difference between the thermal and seismic lithospheric bases of the North China Craton. Chinese Journal of Geophysics (in Chinese) 57 (1), 53–61.
Hopper, J.R., Buck, W.R., 1993. The initiation of rifting at constant tectonic force: Role of diffusion creep. Journal of Geophysical Research 98 (B9), 16213–16221.

Hu, S.B., He, L.J., Wang, J.Y., 2001. Compilation of heat flow data in the China continental area (3rd edition). Chinese Journal of Geophysics 44 (5), 611–626.
Huang, F., He, L.J., Wu, Q.J., 2015. Lithospheric thermal structure of the Ordos Basin and its implications to destruction of the North China Craton. Chinese Journal of Geophysics (in Chinses) 58 (10), 3671–3686.
Huang, H.B., Qiu, X.L., Xia, S.H., 2012. Crustal structure and Poisson's ratio beneath Hainan Island. Journal of Tropical Oceanography 31 (3), 65–70.
Jaupart, C., Mareschal, J.C., Schubert, G., 2007. Heat flow and thermal structure of the lithosphere. Treatise on Geophysics 6, 217–252.
Jia, R., Zhao, D., Wu, J., 2022. P-wave anisotropic tomography of NE China: insight into lithospheric deformation, mantle dynamics and intraplate volcanism. Geophysical Journal International 229, 1372–1391.
Kirby, S.H., 1983. Rheology of the lithosphere. Reviews of Geophysics 21 (6), 1458.
Lavier, L.L., Steckler, M.S., 1997. The effect of sedimentary cover on the flexural strength of continental lithosphere. Nature 389 (6650), 476–479.
Lei D, Pan L Y, Chen Q, et al. Geological characteristics and potential of geothermal resources in the uplift mountain-type of Hainan Island [Online]. Geological Bulletin of China, 1-14.
Li, K.F., Zhu, C.Q., Ma, Z., et al., 2024. Characteristics of thermal physical properties of rocks in Hainan Island and its impact on geothermal field [Online]. Acta Geologic Sinica 1–21. https://doi.org/10.19762/j.cnki.dizhixuebao.2023085.
Liang, X., Zhao, D., Xu, Y., et al., 2022. Anisotropic tomography and dynamics of the big mantle wedge. Geophysical Research Letters 49 (5), e2021GL097550.
Liu, S.W., Wang, L.S., Gong, Y.L., et al., 2005. Thermo-rheological structure of the lithosphere and geodynamics in the Jiyang Depression. Science in China Series D: Earth Sciences 35 (3), 203–214.
Liu, S.W., Wang, L.S., Li, C., et al., 2003. Thermo-rheological structure of the lithosphere and geodynamics in the northern Tarim Basin. Science in China Series D: Earth Sciences 33 (9), 852–863.
Luo, L.U., Wu, C., B, J., 2024. Research on the development of geothermal resources in the northern region of the South China Sea: A case study of Sinopec. Renewable Energy Technology 5 (02), 56–60.
Metcalfe, I., 1996. Gondwanaland dispersion, Asian accretion and evolution of eastern Tethys. Australian Journal Earth Sciences 43 (6), 605–623.
Nolet, G., Zielhuis, A., 1994. Low S velocities under the Tornquist-Teisseyre zone: evidence for water injection into the transition zone by subduction. Journal of Geophysical Research Solid Earth 99 (B8), 15813–15820.
Pollack, H.N., Chapman, D.S., 1977. On the regional variation of heat flow, geotherms, and lithospheric thickness. Tectonophysics 38 (3), 279–296.
Qi, Z.X., Wen, S.N., Pang, C.J., et al., 2023. Formation of Middle-Triassic A-type granites in Northern Hainan Island and its geological implications. Geochimica 52 (1), 69–83.
Qian, Y.S., Zhang, Y.J., Sun, S.Y., 2024. Microseismic analysis and magnitude prediction based on Haikou EGS site in Haikou. Hainan. World Geology 43 (01), 128–135.
Qiu, N.S., Tang, B.N., Zhu, C.Q., 2022. Deep thermal background of hot spring distribution in the Chinese continent. Acta Geological Sinica 96 (1), 195–207.
Qiu, N.S., Xu, W., Zou, Y.H., et al., 2017. Evolution of Meso-Cenozoic thermal structure and thermo-rheological structure of the lithosphere in the Bohai Bay Basin, eastern North China Craton. Earth Science Frontiers 24 (3), 13–26.
Ranalli, G., Murphy, D.C., 1987. Rheological stratification of the lithosphere. Tectonophysics 132 (4), 281–295.
Ranalli, G., 1995. Rheology of the Earth, Second ed. Chapman and Hall, New York.
Rybach, L., Buntebarth, G., 1984. The variation of heat generation, density and seismic velocity with rock type in the continental lithosphere. Tectonophysics 103 (1–4), 335–344.
Shan, J.N., Zhang, G.C., Wu, J.F., et al., 2011. Thermal structure and Moho temperature of Qiongdongnan Basin, Northern Margin of the South China Sea. Chinese Journal of Geophysics (in Chinese) 54 (8), 2102–2109.
Shapiro, N.M., Ritzwoller, M.H., 2004. Thermodynamic constraints on seismic inversions. Geophysical Journal International 157 (3), 1175–1188.
Shi, H.C., Xie, H., Zhao, W.N., Liu, T.W., et al., 2022. Denudation history of Northern Hainan Island since Late Mesozoic-Cenozoic: Evidence from low-temperature thermochronology. Journal of Guangdong Ocean University 42 (1), 78–89.
Shi X M. 2015. Study on the Characteristics of Geothermal Fields and the Flow-Temperature Coupling Model in the Northern Hainan Basin [Ph. D. thesis] (in Chinese). Xuzhou: China University of Mining and Technology.
Sibson, R.H., 1974. Frictional constraints on thrust, wrench and normal faults. Nature 249 (5457), 542–544.
Sobolev, S.V., Zeyen, H., Stoll, G., et al., 1996. Upper mantle temperatures from teleseismic tomography of French Massif Central including effects of composition, mineral reactions, anharmonicity, anelasticity and partial melt. Earth Planetary Science Letters 139 (1–2), 147–163.
Tang, X.Y., Hu, S.B., Zhang, G.C., et al., 2014. Characteristic of surface heat flow in the Pearl River Mouth Basin and its relationship with thermal lithosphere thickness. Chinese Journal of Geophysics (in Chinese) 57 (6), 1857–1867.
Tang, X.Y., Huang, S.P., Zhang, G.C., et al., 2018. Lithospheric thermal structure of Pearl River Mouth Basin, northern South China Sea. Chinese Journal of Geophysics (in Chinses) 67 (9), 3749–3759.
Tang, X.Y., Rao, S., Shan, J.N., et al., 2011. The present geothermal field of Yinggehai Basin. The 27th Annal Meeting of the Chinese Geophysical Society. The Chinese Geophysics 218.
Tesauro, M., Kaban, M.K., Cloetingh, S.A.P.L., 2009. A new thermal and rheological model of the European lithosphere. Tectonophysics 476 (3–4), 478–495.
Wang, C., Wei, C.X., Yun, P., et al., 2019. Zircon U-Pb age, geochemistry and geological significance of Shunzuo granite in Wuzhishan area. Hainan Island. Geological Bulletin of China 38 (8), 1352–1361.
Wang, J.Y., 1996. Geothermics in China. Seismological Press, Beijing.
Wang, Y., 2001. Heat flow pattern and lateral variations of lithosphere strength in China mainland: constraints on active deformation. Physics of the Earth Planetary Interiors 126 (3–4), 121–146.
Wu, D., Li, X.L., Liu, S.W., et al., 2022. Geothermal regime of the deep area of the Qiongdongnan Basin, Northern continental margin of the South China Sea. Geological Journal of China Universities 28 (6), 933–942.
Xia, B.D., Shi, G.Y., Fang, Z., et al., 1991. The late Paleozoic rifting in Hainan Island. China. Acta Geologic Sinica 02, 103–115.
Xia, S.H., Zhao, D.P., Sun, J.L., et al., 2016. Teleseismic Imaging of the Mantle beneath Southernmost China: New Insights into the Hainan Plume. Gondwana Research 36, 46–56.
Xie, Z.F., 2006. Study on seismic activity of Hainan Peninsular and its adjacent area. Technology for Earthquake Disaster Prevention 1 (4), 326–336.
Xu, X.F., Wang, H.L., Chen, X.M., 2014. Analysis on accurate location of earthquake and fault structure in Hainan Island and its adjacent areas. Journal of Seismological Research 37 (2), 216–221+323.
Yang, P., Liu, S.W., 2022. Thermal structure of the continental lithospheric in southeast China and its tectonic implications. Geological Journal of China Universities 28 (5), 698–708.
Yang, P., Liu, S.W., 2024. Heterogeneities of the lithospheric thermal structure and rheology control Cenozoic intracontinental deformation in southeast China. Tectonophysics 870, 230153.
Yun, X.R., Zhang, Y., liang, D.Y., et al., 2023. Granite thermal reservoirs in Lingshui area of Hainan Island and their significance to geothermal resources, China. Energy Geoscience, 100166.
Zang, S.X., Liu, Y.G., Ning, J.Y., 2002. Thermal structure of the lithosphere in north China. Chinese Journal of Geophysics (in Chinses) 45 (1), 56–66.
Zhang, F., Wu, Q., Li, Y., et al., 2019. The seismic evidence of velocity variation for Changbaishan volcanism in Northeast China. Geophysical Journal International 218, 283–294.
Zhang, J., Wang, B.Y., Tang, X.C., et al., 2018. Temperature structure and dynamic background of crust and mantle beneath the high heat flow area of the South China continental margin. Chinese Journal of Geophysics (in Chinese) 61 (1), 3917–3932.
Zhang, J., Wang, J.Y., 2000. The deep thermal characteristic of continental margin of the northern South China Sea. Chinese Science Bulletin 45 (10), 1095–1100.
Zhang, Q., Wu, X.J., Xie, S.S., et al., 2015. Application of Integrated Geophysical Methods in the Exploration of Hot Dry Rock Resources in Lingshui Area, Hainan Province. Chinese Journal of Engineering Geophysics 12 (4), 477–483.
Zhang, Y.P., Li, Q.H., Yu, S.W., 2024. Hydrochemical Characteristics and Identification of the Circulation and Evolution Process of Geothermal Water in the Guantang Area on the East Coast of Hainan Island. Earth Science 49 (3), 952–964.
Zhang Y. 2020. Study on the Characteristics and Genesis of Hot Springs on Hainan Island [Ph. D. thesis] (in Chinese). Beijing: China University of Geosciences (Beijing).
Zhao T. 2016. Characteristics and Evaluation of Geothermal Resources in Hainan Province [Ph. D. thesis] (in Chinese). Guilin: Guilin University of Technology.
Zhou, Y., Zhao, Y.S., Du, Y.J., et al., 2021. Identification of early Paleozoic andesite in Northwestern Hainan Island and its geotectonic significances. Earth Science 46 (11), 3850–3860.